Near Fields of a Log-Periodic Dipole Antenna : NEC Modelling and Comparison with Measurements

K T Wong and P S Excell
Schools of Electrical & Electronic Engineering, University of Bradford, West Yorkshire, BD7 1DP, U.K.

Abstract

Experiences of modelling a log-periodic antenna (tapered transmission line type) using NEC are reported. The antenna is required as a component of a near-field EMC test range, and hence computation of the near fields was the primary objective although some discussion of impedance is presented.

Measurements of the near field of the real antenna were undertaken on a planar measurement range having the ability to scan planes at varying distances from the antenna. The measurements show good agreement with the predictions of NEC.

Introduction

As part of a programme to investigate design parameters for low-cost compact ranges for EMC testing [1,2], the use of an array of seven broadband elements in a hexagonal array is being investigated. The elements currently being evaluated are log-periodic dipole antennas of a standard type intended to operate over the range from 850 to 1800 MHz (Jaybeam Limited, type 7085). These antennas are of a standard design (Fig. 1), constructed from metal rods and having a tapered (V-shape) transmission line. For ease of construction, all of the radiating elements are made of rods of the same cross-sectional diameter, although this deviates from the ideal for log-periodic antennas.

In order to facilitate rapid prediction of the behaviour of arrays of these antennas, a single example was modelled using NEC [3], concentrating on the near-field distributions, and validated by making direct measurements of the near fields of a real antenna using a three-dimensional Cartesian probe-scanning system in an anechoic chamber [4].

The NEC Model

The radiating elements of the antenna shown in Fig. 1 are cylindrical rods, all having the same constant cross-sectional diameter (9 mm), and the transmission line is a pair of tubes with constant square cross-section (12 mm wide). To model this antenna with NEC, the radiating elements can be represented by wires. The transmission line elements may also be represented by wires, in which case they are modelled by circular wires with a cross-sectional perimeter equal to that of the square (i.e. 7.64 mm radius).

Since the width of the tubes is a relatively large fraction of a wavelength at the upper limit of the operating frequency range, and since the tubes come relatively close together at the feed point, some consideration was given to a more detailed model of the square tubes.

A wire grid model could be used, constructed from eight parallel longitudinal wires connected by a sequence of transverse squares of wire: this approach was rejected due to the very large number of segments that would be required. A representation using surface patches was tried but the results were very unsatisfactory (severe errors in the polarisation of the computed near field) and the approach was abandoned.

The upper and lower halves of the antenna are not mirror images of each other and hence reflection cannot be used to simplify data input. It is, however, possible to model one half of the antenna and then rotate it through 180° about the main lobe axis to generate the lower half.

With the wire model of the transmission line it is not possible to satisfy the criterion for the ratio of segment length (Δ) to wire radius (a) unless the extended thin-wire kernel is used, due to the intricacy of the structure. Even so, it is impossible to avoid Δ/a ratios of somewhat less than the desirable minimum of two in a few segments at the upper limit of the operating frequency range.

The vertical rod joining the ends of the transmission line tubes at the rear of the antenna was modelled as a cylindrical wire, and a segment containing a voltage generator was connected to the front ends of the two transmission line tubes. No attempt was made to model the support structure beyond the vertical rod.

Physical measurements with a planar near-field probe scanner

Near field measurements were carried out in an anechoic chamber containing a probe positioner capable of measuring the field at any point in a cubical volume. In the present case, measurements were performed on two planes oriented normally to the nominal antenna boresight direction at distances of 400 and 800 mm from the feed point of the antenna. The electric field probe used was an electrically-short dipole (46 mm overall length), connected to a coaxial cable via a broadband balun. In practice, it was found that the performance of the balun was not ideal, leading to a certain amount of residual 'boresight error' in the probe at most frequencies. This effect was cancelled out by taking the average of two sets of measurements, the probe being rotated through 180° between each set. The fields were measured over symmetrical one-metre scan widths along the two principal transverse axes only (x and y co-ordinates). The sample spacing used was 100 mm at 850 and 1000 MHz and 50 mm at 1800 MHz. According to the Nyquist sampling criterion, these spacings will resolve evanescent modes with vector wave numbers having imaginary z-components of 25.9 m^{-1}, 23.4 m^{-1} and 50.2 m^{-1} respectively. At the minimum scanning distance of 400 mm, such modes will be attenuated by 90, 81 and 174 dB respectively, compared with their values on the nominal aperture plane passing through the feed point of the antenna. It is thus concluded that the sample spacings used are adequate to resolve the detailed structure of the near field distribution at the distances chosen.

Computation using NEC

Using the input data set generated as described above, NEC was run on an Amdahl 5890-300 computer. The total number of segments used at the three frequencies of interest (for the single wire representation of the transmission line) is shown in Table 1, together with the corresponding CPU times.

Comparison of results

Figures 2 to 4 show the computed and measured results. Only the magnitude of the dominant x-component of the electric field is shown, as this is the most useful for comparison purposes, being directly proportional to the probe output voltage. All of the results shown are normalised to give 0 dB amplitude and 0° phase in the centre of the distribution at Z = 400 mm.

Comparison of the predicted and measured amplitude distributions shows reasonably good agreement, the maximum discrepancy being around 1 dB. The agreement observed between the phase measurements and the NEC predictions is excellent, even in the regions of rapid phase change at the higher frequencies: the maximum phase discrepancy being about 10°.

Table 2 gives a comparison of the VSWR, as calculated from the input impedance predicted by NEC, and the corresponding typical values given by the antenna manufacturer. These figures show remarkably good agreement at lower frequencies, but this deteriorates at the upper end of the range.

Conclusions

The results of computation of the near fields of a log-periodic dipole antenna, using NEC, have been presented and compared with measurements on a real antenna obtained using a planar near-field probe positioner.

Although some doubts were entertained concerning the validity of use of a cylindrical wire model for the square tubes forming the transmission line, the agreement between the measured results and the NEC predictions using the wire representation is very good, showing a maximum error of about 1dB in the amplitude and 10° in the phase. Attempts to use a more detailed model for the transmission line were unsuccessful.

The antenna VSWR deduced from the NEC predictions of the impedance shows good agreement with the manufacturer's typical data for the real antenna although the agreement deteriorates at the upper end of the nominal operating band of the antenna.

Work on the modelling and testing of arrays of these antennas is proceeding.

References

1. Excell, P S and Gunes Z F: 'The compact range principle applied to electromagnetic susceptibility testing', IERE Conf. Pub. No. 56, 'Electromagnetic Compatibility', 1982, pp. 317-322.

2. Excell, P S: 'Assessment of errors in radiative susceptibility and emission testing in a compact range', IERE Conf. Pub. No. 60, 'Electromagnetic Compatibility, 1984, pp. 33-38.

3. Burke, G J and Poggio, A J: 'NEC-Method of Moments', NOSC TD116, 1981.

4. Rousseau, M and Excell, P S: 'Computation of the field distribution in a broadband compact range for EMC applications', IEE Conf. Pub. No. 274, 'Antennas & Propagation', 1987, pp.395-398.

Acknowledgements

This work forms a part of a project funded by the UK Science and Engineering Research Council. The planar probe positioner and its control system were built by Moshe Rousseau.

Appendix

Listing of NEC input deck for LPDA at 1000MHz

(NEC modified for free-format input)

```
CM CALCULATE THE NEAR FIELDS OF A LPDA, WITH THE TRANSMISSION LINE
CM REPRESENTED BY A SERIES OF CIRCULAR RODS, THE ENDS
CM OF THE RODS COINCIDING WITH THE RADIATING ELEMENTS.
CM FREQUENCY = 1000 MHZ
CM RADIUS OF CIRCULAR RODS = 7.64 MM
CE
GW 101 1  0  0.012    -0.040    0       0.01545  -0.06728  0.00764
GW 102 1  0  0.01545 -0.06728   0       0.01777  -0.08564  0.00764
GW 103 1  0  0.01777 -0.08564   0       0.02040  -0.10647  0.00764
GW 104 1  0  0.02040 -0.10647   0       0.02341  -0.13028  0.00764
GW 105 1  0  0.02341 -0.13028   0       0.02654  -0.15509  0.00764
GW 106 1  0  0.02654 -0.15509   0       0.03030  -0.18485  0.00764
GW 107 2  0  0.03030 -0.18485   0       0.03456  -0.21858  0.00764
GW 108 2  0  0.03456 -0.21858   0       0.03888  -0.25281  0.00764
GW 109 2  0  0.03888 -0.25281   0       0.04383  -0.29200  0.00764
GW 110 2  0  0.04383 -0.29200   0       0.04935  -0.33565  0.00764
GW 111 2  0  0.04935 -0.33565   0       0.05537  -0.38327  0.00764
GW 112 2  0  0.05537 -0.38327   0       0.06238  -0.43883  0.00764
GW 113 4  0  0.06238 -0.43883   0       0.07542  -0.54201  0.00764
GW 1    1  0  0.01545 -0.06728 -0.023 0.01545  -0.06728  0.0045
GW 2    1  0  0.01777 -0.08564  0.026 0.01777  -0.08564  0.0045
GW 3    2  0  0.02040 -0.10647 -0.031 0.02040  -0.10647  0.0045
GW 4    2  0  0.02341 -0.13028  0.034 0.02341  -0.13028  0.0045
GW 5    2  0  0.02654 -0.15509 -0.038 0.02654  -0.15509  0.0045
GW 6    2  0  0.03030 -0.18485  0.043 0.03030  -0.18485  0.0045
GW 7    2  0  0.03456 -0.21858 -0.048 0.03456  -0.21858  0.0045
GW 8    3  0  0.03888 -0.25281  0.054 0.03888  -0.25281  0.0045
GW 9    3  0  0.04383 -0.29200 -0.061 0.04383  -0.29200  0.0045
GW 10   3  0  0.04935 -0.33565  0.068 0.04935  -0.33565  0.0045
GW 11   3  0  0.05537 -0.38327 -0.076 0.05537  -0.38327  0.0045
GW 12   4  0  0.06238 -0.43883  0.084 0.06238  -0.43883  0.0045
GM 100     1    0 0 180   0  0  0  0
GW 9999 1 0  -0.012   -0.040    0       0.012    -0.040    0.00732
GW 999 5  0 -0.07542 -0.54201   0       0.07542  -0.54201  0.0125
GE 0 0   0 0 0   0 0 0   0  0
EK 0 0 0 0 0   0 0 0 0 0
FR 0 0  0 0  1000   0 0 0 0 0
EX 0 9999 1 01 1  0 50 0 0 0
NE 0    11 11  2   -0.5 -0.5  0.4    0.1  0.1  0.4
EN 0 0 0 0 0   0 0 0 0 0
```

Table 1: Total CPU Times on Amdahl 5890 - 300

Frequency (MHz)	No. of Segments in model	CPU time (s)
850	102	5.27
1000	106	5.42
1800	153	15.27

Table 2: Comparison of VSWRs derived from NEC with Manufacturer's Typical Data

Frequency (MHz)	VSWR NEC	VSWR Mfr
850	3.8	3.4
1000	3.0	3.0
1100	3.5	2.7
1400	3.3	3.3
1800	2.0	3.5
2000	1.9	3.3

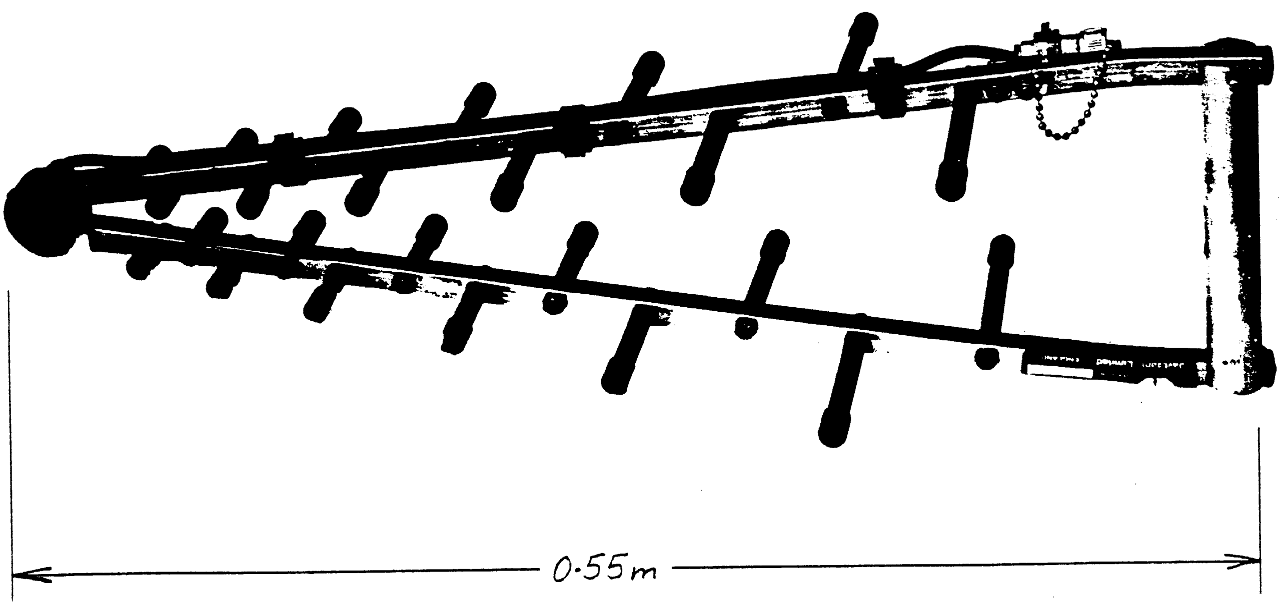

Fig. 1: The log-periodic dipole antenna

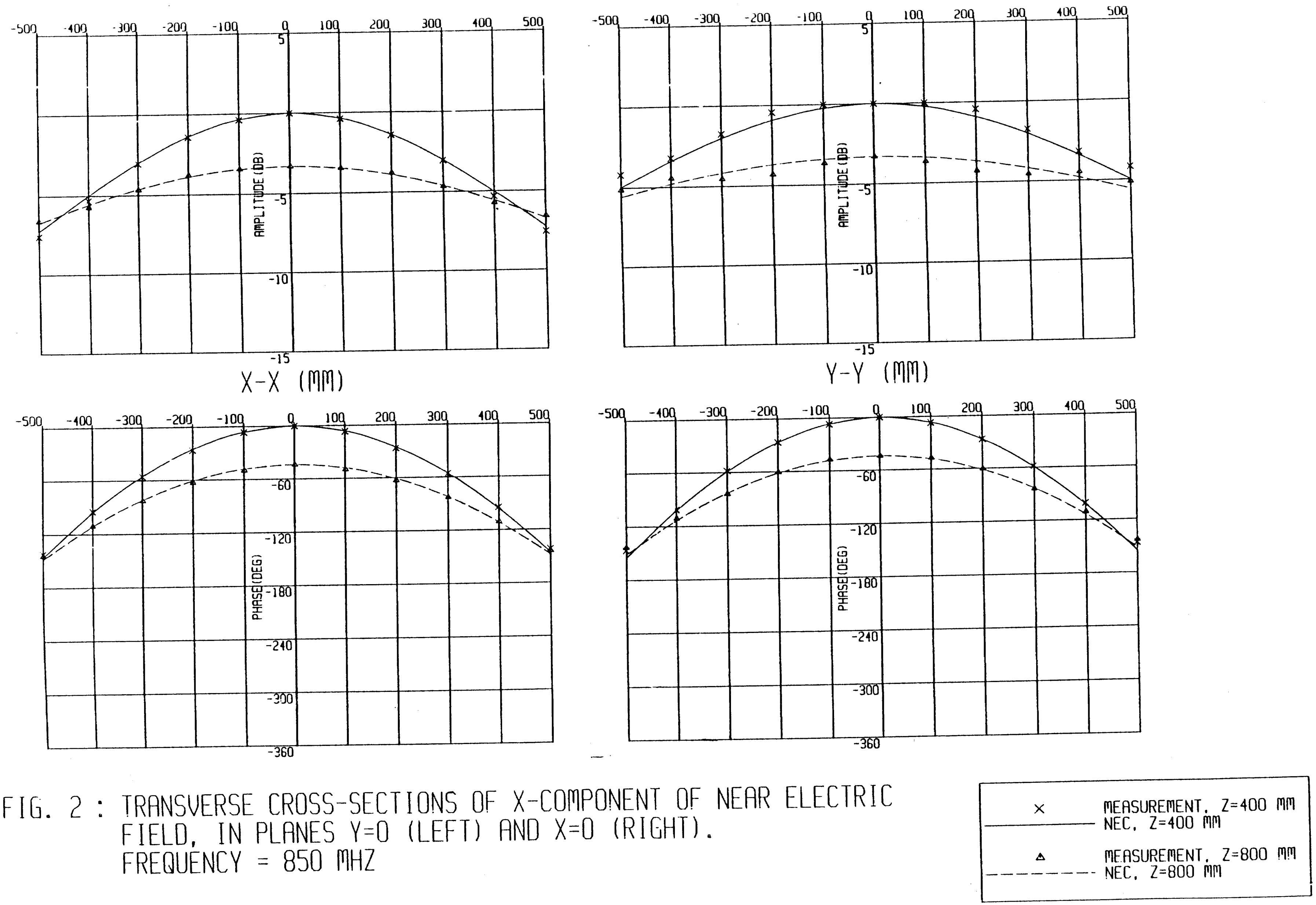

FIG. 2 : TRANSVERSE CROSS-SECTIONS OF X-COMPONENT OF NEAR ELECTRIC FIELD, IN PLANES Y=0 (LEFT) AND X=0 (RIGHT). FREQUENCY = 850 MHZ

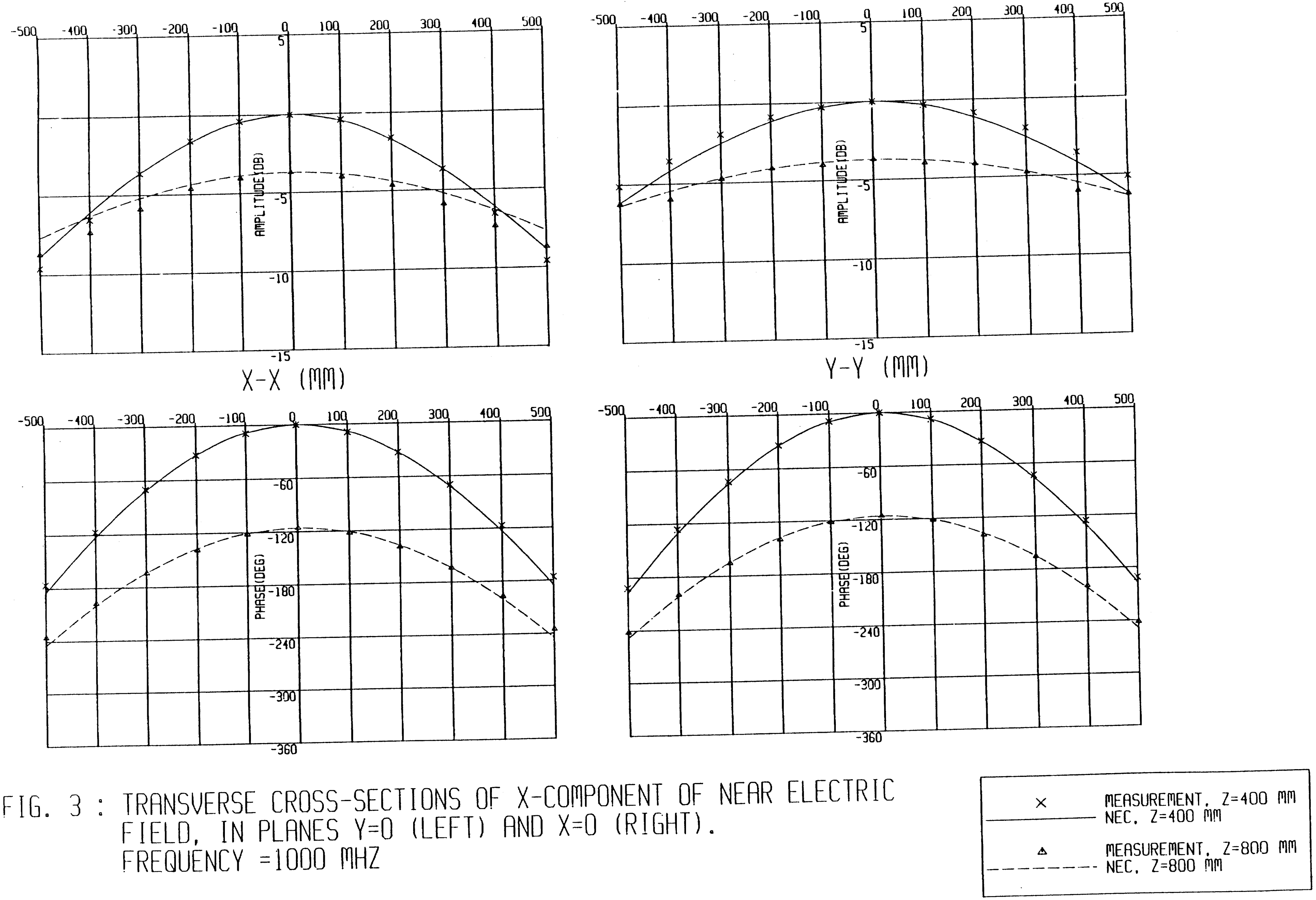

FIG. 3 : TRANSVERSE CROSS-SECTIONS OF X-COMPONENT OF NEAR ELECTRIC FIELD, IN PLANES Y=0 (LEFT) AND X=0 (RIGHT).
FREQUENCY =1000 MHZ

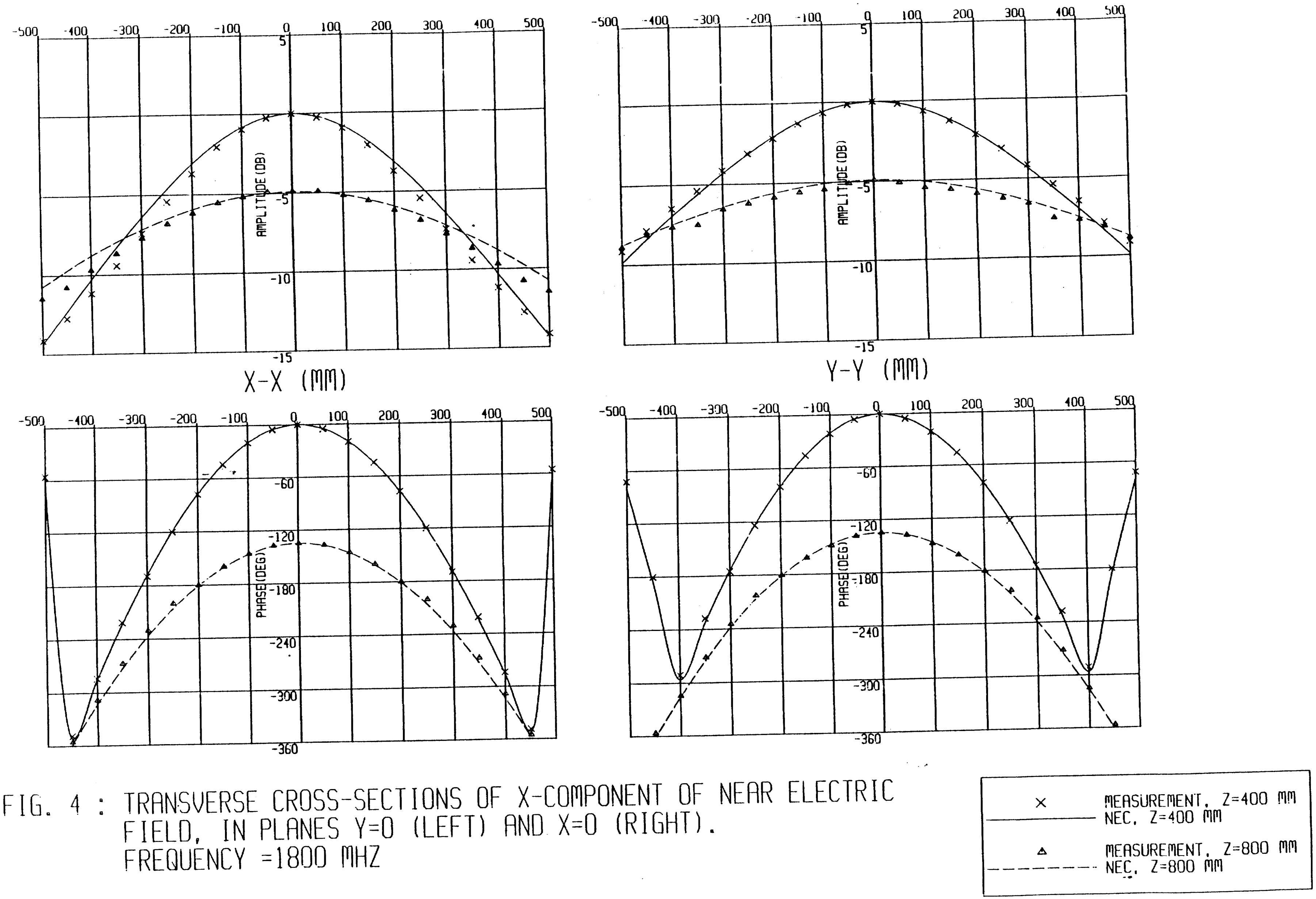

FIG. 4 : TRANSVERSE CROSS-SECTIONS OF X-COMPONENT OF NEAR ELECTRIC FIELD, IN PLANES Y=0 (LEFT) AND X=0 (RIGHT).
FREQUENCY =1800 MHZ